JCI insight

Myokine SIRPα exacerbates kidney disease in diabetes

Jiao Wu, Elisa Russo, Daniela Verzola, Qingtian Li, Helena Zhang, Bhuvaneswari Krishnan, David Sheikh-Hamad, Zhaoyong Hu, William E. Mitch, Sandhya S. Thomas

JCI Insight. 2026;11(3):e183392. https://doi.org/10.1172/jci.insight.183392.

Research Article | Endocrinology | Nephrology

Graphical abstract

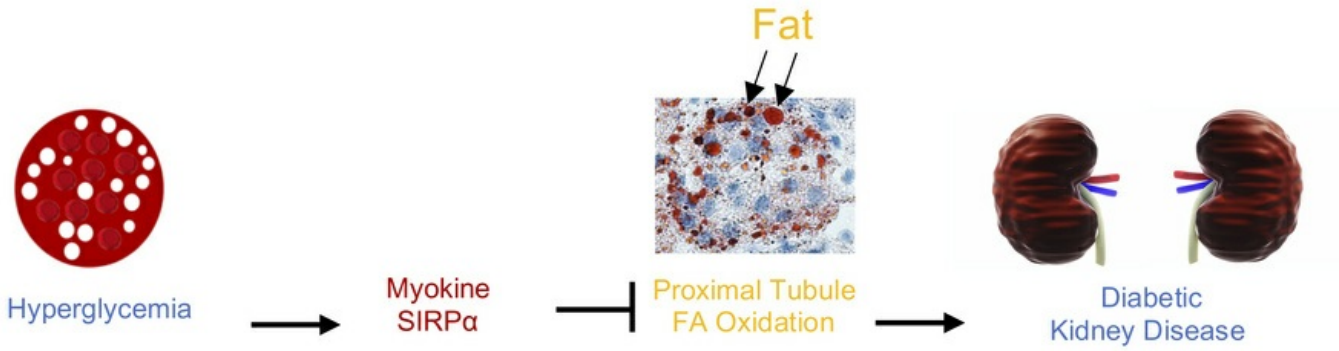

JCI insight

RESEARCH ARTICLE

Myokine SIRPα exacerbates kidney disease in diabetes

Jiao Wu,[1] Elisa Russo,[2] Daniela Verzola,[2] Qingtian Li,[1] Helena Zhang,[1] Bhuvaneswari Krishnan,[3] David Sheikh-Hamad,[1,4] Zhaoyong Hu,[1] William E. Mitch,[1] and Sandhya S. Thomas[1,4]

[1]Nephrology Division, Department of Medicine, Baylor College of Medicine (BCM), Houston, Texas, USA. [2]Nephrology Division, Department of Medicine, Università degli Studi di Genova, Genoa, Italy. [3]Department of Pathology and Immunology, BCM, Houston, Texas, USA. [4]Nephrology Division, Department of Medicine, Michael E. DeBakey VA Medical Center, Houston, Texas, USA.

Mechanisms responsible for skeletal muscle kidney crosstalk have not been defined. We have determined that a circulating mediator, signal regulatory protein α (SIRPα), impairs intracellular insulin-mediated functions. To elucidate the effect of myokine SIRPα on diabetic kidney disease (DKD), flox mice and muscle-specific (m-specific) SIRPα-KO mice were subjected to an obesity-induced model of diabetes, high-fat diet (HFD; 60%) or insulin-deficient hyperglycemia model, streptozotocin (STZ), and were subsequently exposed to anti-SIRPα monoclonal antibodies. In the obesity-induced diabetic mice, serum SIRPα increased. Genetic deletion of muscle SIRPα protected against obesity and improved intracellular insulin signaling in muscle and adipose tissue, with reduced intramuscular fat deposition when compared with *flox* mice on HFD. Moreover, *mSIRPα*-KO mice displayed enhanced kidney tubular fatty acid oxidation (FAO) expression with suppressed intraorgan triglycerides deposition, and importantly, protection against DKD. Conversely, exogenous SIRPα impaired kidney proximal tubular cell FAO, ATP production, and exacerbated fibrosis. Finally, suppressing SIRPα in skeletal muscles or treatment with anti-SIRPα monoclonal antibodies in STZ-treated mice mitigated cachexia, hyperlipidemia, kidney triglyceride deposition, and renal dysfunction in spite of significant hyperglycemia. Importantly, serum SIRPα was upregulated in patients with DKD. In conclusion, SIRPα serves as a potential biomarker and therapeutic target in DKD.

Introduction

Chronic kidney disease (CKD) affects an estimated 15% (~37 million or 1 in 7) of US adults according to the Centers for Disease Control and Prevention (CDC) (1, 2). Patients with CKD display evidence of systemic insulin resistance with or without diabetes (3). We have determined that signal regulatory protein α (SIRPα) is responsible for postinsulin receptor defects impairing intracellular insulin signaling in a subtotal nephrectomy model of CKD (4). Specifically, SIRPα reduces tyrosine phosphorylation of insulin substrate 1 (IRS1), insulin receptor, or insulin-like growth factor-1 (IGF-1) receptor in skeletal or cardiac muscle contributing to peripheral organ insulin resistance in CKD (4, 5). Moreover, SIRPα affects insulin signaling in CKD, contributing to pathologic browning and skeletal muscle loss (6). Therefore, we examined the influence of SIRPα in diabetic kidney disease (DKD).

The muscle plays a critical role in kidney function, details of which are underrecognized. In fact, creatinine, a product of muscle tissue breakdown, is utilized for measurements of kidney function (7). Moreover, circulating myokines may be responsible for improved or worsening kidney disease. For example, myostatin has been implicated in worsening interstitial fibrosis in diabetic nephropathy (8). Additionally, exercise-associated myokines (i.e., irisin) are involved in muscle-kidney crosstalk, suppressing metabolic reprogramming and the development of kidney fibrosis (9). Skeletal muscle–specific Akt1 transgenic mice prevented skeletal muscle loss with improved kidney function despite the presence of unilateral ureteral obstruction (UUO) (10). In fact, aerobic exercise (e.g., walking) revealed benefits in cardiovascular health in predialysis patients with CKD (11–13).

Hyperglycemia alone may not correlate with worsening DKD; moreover, lower hemoglobin A1c levels < 6.5% correlated with worsening patient outcomes (14, 15). Thus, it is possible that pathologic myokines may be contributing to worsening kidney function irrespective of glucose controls. We have determined that

Conflict of interest: The authors have declared that no conflict of interest exists.

Submitted: June 20, 2024
Accepted: December 9, 2025
Published: February 9, 2026

Reference information: *JCI Insight*. 2026;11(3):e183392. https://doi.org/10.1172/jci.insight.183392.

exposure to hyperglycemia or uremic toxins stimulates SIRPα release into cultured myocyte media but not cultured adipocyte media (8). Additionally, control mice exposed to acute hyperglycemia stimulates increased serum SIRPα (8). Furthermore, patients with CKD display an increase in serum SIRPα when compared with healthy controls (8). Therefore, in this study, we examined the effects of SIRPα responses in DKD.

DKD is associated with alterations in kidney tubular FAO, but the mechanisms responsible for insulin resistance–induced impaired FAO have not been elucidated (16). FAO is a preferred mitochondrial respiratory substrate for highly metabolic cells, including cardiomyocytes and kidney proximal tubular cells (17). The kidney is second only to cardiac muscle in mitochondrial numbers and oxygen consumption (17, 18). ATP generation in the proximal tubular cells occurs mainly through fatty acid oxidation (17). Lipotoxicity has been linked to advancing kidney disease (19). Kang et al. determined that overexpression of long-chain fatty acid transporter CD36 contributed to lipid accumulation in renal tubular epithelial cells but did not directly lead to renal fibrosis (20). Therefore, the investigators concluded that lipid accumulation was not the main factor responsible for kidney dysfunction. In fact, reduced FAO or fatty acid utilization has been linked to the development of tubulointerstitial fibrosis via TGF-β1 (20). Specifically, impaired FAO induces ATP depletion, tubular necrosis, maladaptive repair, and ultimately kidney dysfunction (20). Here we examined the effect of a mediator of insulin signaling, myokine SIRPα, on kidney FAO and the importance of muscle-kidney crosstalk in DKD.

Results

Obesity-induced hyperglycemia stimulates serum SIRPα, while suppression of SIRPα initiates salutary effects on diet-induced obesity. In order to establish organ-specific SIRPα effects in diabetic disease, muscle-specific SIRPα knockout (KO, $^{-/-}$) mice were created and fed a 60% high-fat diet (HFD) and compared with normal chow–fed (NC-fed) mice. Serum SIRPα was found to be significantly increased in *flox* mice on HFD, but serum SIRPα was not increased in muscle-specific SIRPα-KO (*mSIRPα*$^{-/-}$) mice on HFD based on ELISA (Figure 1A) and Western blot measurements (Supplemental Figure 1A; supplemental material available online with this article; https://doi.org/10.1172/jci.insight.183392DS1). These results were associated with improved glucose tolerance test (GTT) and insulin tolerance test (ITT) in *mSIRPα*$^{-/-}$ mice on HFD compared with *flox* mice on HFD at 9 weeks and 11 weeks, respectively (Figure 1, B and C), although these differences did not persist beyond 13 weeks (Supplemental Figure 1, B and C), while displaying similar fasting insulin levels in *flox* mice and *mSIRPα*$^{-/-}$ mice on HFD at 14 weeks (Figure 1D).

In gastrocnemius (GAS) skeletal muscle and epididymal white adipose tissue (eWAT), *flox* mice on HFD displayed upregulation of SIRPα proteins with suppressed activation of pAKT (ser 476) signaling (Figure 1, E and F); no differences were noted in intracellular insulin signaling in GAS muscle and eWAT of *mSIRPα*$^{-/-}$ on HFD when compared with their respective control mice on NC while intracellular signaling was improved when compared with *flox* mice on HFD (Figure 1, E and F). Results presented here suggest that the obesity model of type 2 diabetes stimulates increases in serum SIRPα while muscle-specific SIRPα KO leads to improved intracellular insulin signaling in muscle and fat despite HFD feeding. Compared with *flox* mice, obesity was suppressed in *mSIRPα*$^{-/-}$ mice despite HFD beginning at 6 weeks, and these suppressed weight changes persisted until 14 weeks (Figure 1G).

Next, organ weights were evaluated, and *mSIRPα*$^{-/-}$ mice displayed improved inguinal WAT (iWAT), eWAT, and liver weights after HFD feeding when compared with *flox* mice on HFD (Supplemental Figure 1D). These differences were identified despite similar food and water intake (Supplemental Figure 2A). Finally, except for day RER (VCO_2/VO_2), no significant differences were identified in VO_2, VCO_2, night RER, heat production or activity counts when comparing *flox* vs. *mSIRPα*$^{-/-}$ on HFD (Supplemental Figure 2, B–F). In summary, SIRPα suppression in muscle led to improvements in body and organ weights despite HFD-feed and hyperinsulinemia.

HFD suppresses FAO genes in adipose tissue while influencing adipokines. Next, the effects of SIRPα on eWAT were evaluated in response to obesity-induced diabetes. In *flox* mice, HFD increased eWAT adipocyte area when compared with mice on NC (Figure 2A). However, *mSIRPα*$^{-/-}$ mice on HFD displayed improved adipocyte area similar to *mSIRPα*$^{-/-}$ mice on regular chow (Figure 2A). HFD-fed *flox* mice displayed reduced expression of the thermogenin protein, UCP1, in eWAT when compared with NC-fed *flox* mice, while *mSIRPα*$^{-/-}$ mice on HFD feed showed preservation of UCP1 expression when compared their respective controls (Figure 2B). Additionally, genes *Ppargc1a* encoding PGC1α and *Ppara* encoding PPARα were suppressed in eWAT in response to HFD in *flox* mice but not *mSIRPα*$^{-/-}$ mice on HFD (Figure 2C). Next, we examined

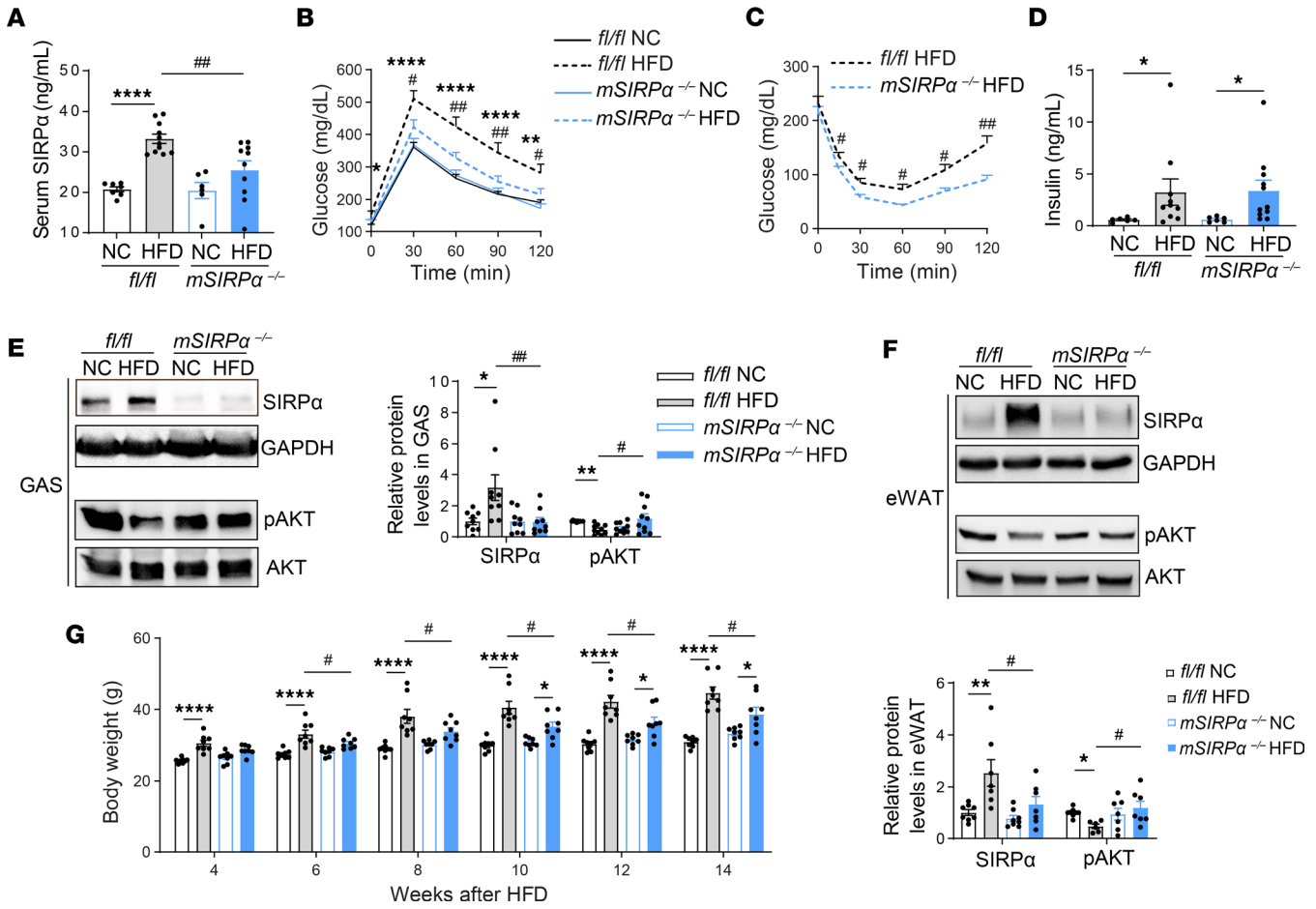

Figure 1. Blocking SIRPα in muscle prevents serum SIRPα release while improving insulin sensitivity in an obesity model of type 2 diabetes. Five-week-old *fl/fl*, muscle-specific SIRPα-KO (*mSIRPα*$^{-/-}$) mice were fed with high-fat diet (HFD) vs. normal chow (NC) diet for 16 weeks. (**A**) Serum SIRPα was confirmed by ELISA (n = 6–11). (**B**–**D**) Glucose tolerance (n = 7–10), insulin tolerance (n = 6–9), and insulin levels (after 16 hours fasting) were measured (n = 6–11). (**E** and **F**) Representative immunoblots for SIRPα, pAKT and AKT in gastrocnemius (GAS, n = 9-10) skeletal muscle and epididymal white adipose tissue (eWAT, n = 6-8) are shown. The relative SIRPα to GAPDH or pAKT to AKT levels are shown. (**G**) Mice body weights (BW) were determined (n = 8). Data are shown as mean ± SEM. Statistical significance analysis was performed using 2-tailed unpaired t test for **C**; 1-way ANOVA followed by Bonferroni test for **A**, **B**, and **G** and SIRPα in **F**; and Kruskal-Wallis test followed by Dunn's multiple comparisons for **D** and **E** and pAKT in **F**. *P < 0.05, **P < 0.01, ****P < 0.0001 NC vs. HFD; $^{\#}P$ < 0.05, $^{\#\#}P$ < 0.01 *fl/fl* vs. *mSIRPα*$^{-/-}$.

adipokine responses; when comparing eWAT of *flox* mice HFD-fed and *flox* NC-fed mice, we observed a reduction in the gene *Adipoq* encoding adiponectin (important for insulin sensitivity) plus an upregulation of *Lep* encoding the satiety hormone leptin (Figure 2D). In contrast, both adiponectin and leptin mRNA levels were unchanged in *mSIRPα*$^{-/-}$ mice on HFD when compared with the NC-fed mice. In fact, *Adipoq* was improved while *Lep* was suppressed in *mSIRPα*$^{-/-}$ mice vs. *flox* mice on HFD (Figure 2D). Similarly, eWAT of HFD-fed *flox* mice displayed increased expression of the adipokine TSP1 (associated with obesity and insulin resistance) but was unchanged in eWAT of HFD-fed *mSIRPα*$^{-/-}$ mice (Figure 2E). Therefore, factors influencing diabetic changes in eWAT were improved in *mSIRPα*$^{-/-}$ mice on HFD.

SIRPα knockdown improves muscle quality despite hyperglycemia. Skeletal muscle dysfunction is critical to the development of diabetes; therefore, skeletal muscle quality and function were evaluated in response to obesity-induced diabetes. In response to HFD, *flox* mice displayed worsening grip strength and skeletal muscle wasting in both GAS and tibialis anterior (TA) muscle (Figure 3, A–C). However, *mSIRPα*$^{-/-}$ mice vs. *flox* mice on HFD displayed improved grip strength, GAS, and TA skeletal muscle weights (Figure 3, A–C). Cross-sectional areas (CSA) of the TA muscle were reduced in response to HFD in *flox* mice with a leftward shift of CSA but improved in HFD-fed *mSIRPα*$^{-/-}$ with a rightward shift on CSA (Figure 3D). These results were associated with an upregulation in mRNA transcripts responsible for muscle protein degradation E3 ubiquitin ligases, MuRF1 (*Trim63*),

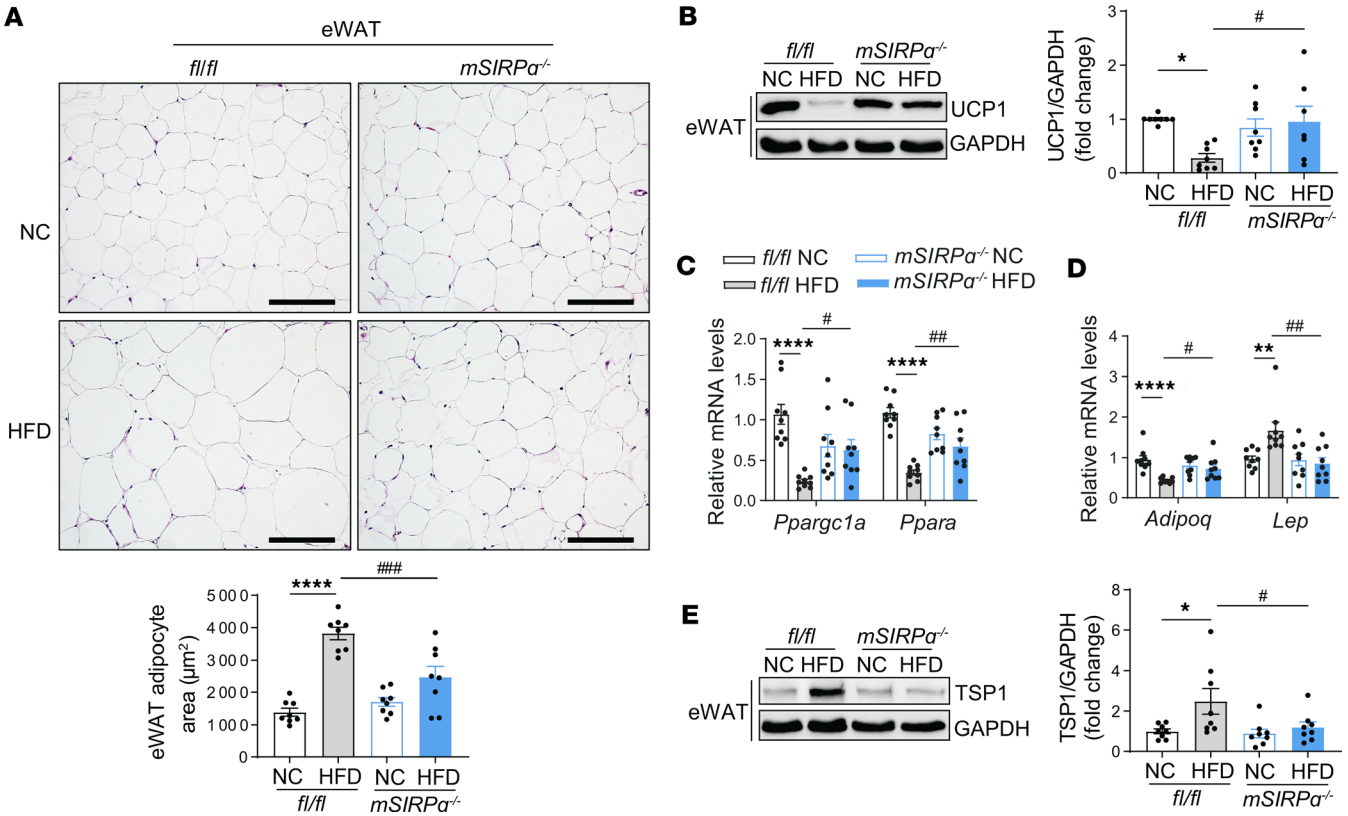

Figure 2. Blocking SIRPα in muscle improves white adipose tissue metabolism. Five-week-old *fl/fl*, muscle-specific SIRPα-KO (*mSIRPα*$^{-/-}$) mice were fed with high-fat diet (HFD) vs. normal chow (NC) diet for 16 weeks. (**A**) Representative H&E-stained epididymal white adipose tissue (eWAT) was obtained and eWAT adipocyte area was measured (scale bar: 100 μm, *n* = 8). (**B**) Representative immunoblots for UCP1 in eWAT and relative densities to GAPDH (*n* = 7–8). (**C**) Relative mRNA fatty oxidation transcript levels were determined in eWAT by qPCR (*n* = 9). (**D**) Relative mRNA levels of adiponectin (*Adipoq*) and leptin (*Lep*) were identified in eWAT by qPCR (*n* = 9). (**E**) Representative immunoblots of adipokine TSP1 in eWAT and the relative densities to GAPDH (*n* = 8). Data are shown as mean ± SEM. Statistical significance was performed using 1-way ANOVA followed by Bonferroni test for **A**–**E**. **P* < 0.05, ***P* < 0.01, *****P* < 0.0001 NC vs. HFD; #*P* < 0.05, ##*P* < 0.01, ###*P* < 0.001 *fl/fl* vs. *mSIRPα*$^{-/-}$.

and Atrogin-1 (*Fbxo32*) in *flox* mice on HFD with suppression of skeletal muscle E3 ubiquitin ligases in HFD-fed *mSIRPα*$^{-/-}$ (Figure 3E). This is relevant, as these E3 ubiquitin ligase elevations have been associated with muscle protein degradation and atrophy. Of interest, intramuscular lipid was increased in HFD-fed *flox* mice but significantly suppressed in HFD-fed *mSIRPα*$^{-/-}$ (Figure 3F). Thus, blocking muscle SIRPα protected against loss of grip strength and ectopic skeletal muscle lipid deposition, and prevented skeletal muscle wasting despite HFD-feed exposure.

Obesity-induced diabetes suppresses kidney tubular FAO. Therefore, because a reduction in kidney epithelial tubular FAO was noted in patients with hypertensive-diabetic CKD (20), we examined kidney FAO in the HFD model-inducing DKD. Specifically, we evaluated myokine SIRPα effects on kidney epithelial tubular cells. Polyuria, albuminuria, serum creatinine, serum cystatin C, and glomerular area were increased in HFD-fed *flox* mice while suppressed in *mSIRPα*$^{-/-}$mice despite high-fat feeds (Figure 4, A–E). Kidney fibrosis — based on sirius red staining, mRNA transcripts of collagen I (*Col1a1*), fibronectin (*Fn1*), and immunoblots for fibronectin and α smooth muscle actin (αSMA; Figure 4, F–H) — were increased in HFD-fed *flox* mice but not HFD-fed *mSIRPα*$^{-/-}$ mice when compared with their respective controls with improvements in sirius red staining area plus fibrosis-related mRNA transcripts and protein levels in *mSIRPα*$^{-/-}$ mice vs. *flox* mice on HFD (Figure 4, F–H).

Next, glucosuria was increased in HFD-fed *flox* mice but not in *mSIRPα*$^{-/-}$ mice with HFD (Supplemental Figure 3A). No differences were noted in systolic blood pressure (BP) in these mice (Supplemental Figure 3B). Moreover, kidney IL-6 (*Il6*) transcripts were upregulated in HFD-fed *flox* mice vs. control mice, but not in *mSIRPα*$^{-/-}$ mice on HFD, while TNF-α (*Tnf*) was upregulated in *flox* mice on HFD when compared with *mSIRPα*$^{-/-}$ mice on HFD (Figure 4G). Importantly, kidney triglyceride (TG) concentration was found to be significantly increased in HFD-fed *flox* mice, which was significantly reduced in

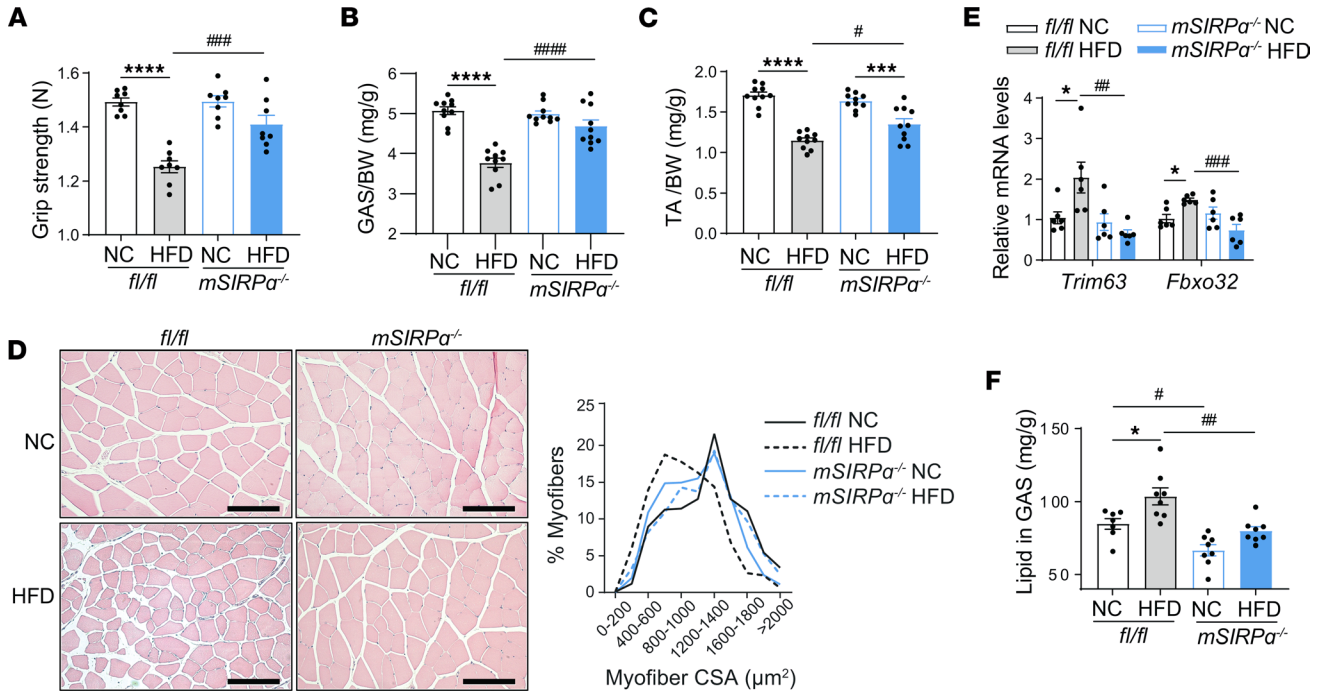

Figure 3. Blocking muscle SIRPα suppresses ectopic lipid accumulation while attenuating skeletal muscle wasting in obesity-induced diabetes. (**A**) After 14 weeks of high-fat diet (HFD) or normal chow (NC) diet, grip strength (Newtons [N]) was measured in *fl/fl*, muscle-specific SIRPα-KO (*mSIRPα*$^{-/-}$) mice (n = 8). (**B** and **C**) Gastrocnemius (GAS) and tibialis anterior (TA) skeletal muscles were weighed and normalized to body weight (BW; n = 10). (**D**) Representative H&E-stained cryosections of TA skeletal muscle (scale bar: 100 μm) and percentage (%) of myofiber sizes are shown (n = 3–4). (**E**) Relative mRNA levels of atrophy-related transcripts were determined in gastrocnemius muscle by qPCR (n = 6). (**F**) Total lipid concentration was identified in gastrocnemius skeletal muscle (n = 7–8). Data are shown as mean ± SEM. Statistical significance was performed using one-way ANOVA followed by Bonferroni test for **A**–**C**, **E**, and **F**. $^{*}P < 0.05$, $^{***}P < 0.001$, $^{****}P < 0.0001$ NC vs. HFD; $^{\#}P < 0.05$, $^{\#\#}P < 0.01$, $^{\#\#\#}P < 0.001$, $^{\#\#\#\#}P < 0.0001$ *fl/fl* vs. *mSIRPα*$^{-/-}$.

HFD-fed *mSIRPα*$^{-/-}$ mice (Figure 4I). Additionally, genes encoding FAO transcripts (*Ppargc1a*, *Pparg*, *Cpt1a*, *Acox1*) were suppressed in HFD-fed *flox* mice but remained unchanged in *mSIRPα*$^{-/-}$ mice on HFD when compared with their respective controls (Figure 4J). In fact, FAO transcripts were significantly improved in *mSIRPα*$^{-/-}$ mice vs. *flox* mice on HFD (Figure 4J). Finally, SIRPα protein was upregulated in kidneys of *flox* mice on HFD (Figure 4K). In brief, suppressing muscle SIRPα prevented renal fibrosis and changes in fatty acid metabolism while maintaining kidney function in an obesity model of diabetes.

Exogenous SIRPα suppresses kidney tubular epithelial cells FAO. Next, we examined the oxygen consumption rates (OCR) of cultured kidney tubular cells to quantitatively analyze renal proximal tubular metabolism exposed to hyperglycemia or recombinant SIRPα (rSIRPα) protein (Figure 5A). Mouse proximal tubule–derived cell line, BUMPT cells, were treated with a 3-fold higher glucose concentration (75 mM) and compared with standard glucose media (25 mM). High glucose–treated cells had evidence of reduced OCR including basal, maximal, and ATP-linked OCR (Figure 5, A and B). These results were associated with decreased mRNA transcripts encoding FAO (Figure 5C). Next, to determine if exogenous SIRPα directly affects renal proximal tubular FAO, BUMPT cells were exposed to rSIRPα protein. Similar to high glucose–treated cells, rSIRPα-treated cells had evidence of reduced OCR including reduced basal, maximal and ATP-linked OCR similar to high glucose–treated cells (Figure 5, A and B). These outcomes were associated with a reduction in transcript levels for genes encoding FAO in rSIRPα-treated cells (Figure 5D).

Additionally, BUMPT cells were treated at varying concentrations of glucose — 5.5 mM (low) vs. 25 mM (standard) — and OCR were evaluated. Compared with 5.5 mM glucose, 25 mM glucose-treated cells had evidence of reduced OCR including basal, maximal, and ATP-linked OCR (Supplemental Figure 4, A and B). These result findings of 5.5 vs. 25 mM glucose-treated cells were associated with decreased mRNA transcripts encoding FAO (Supplemental Figure 4C).

Next, both primary proximal tubular cells isolated from *flox* control mice kidney cortex (Figure 5, E–G, and Supplemental Figure 4D) and BUMPT cells (Supplemental Figure 4E) were examined after rSIRPα treatment; lipid accumulation was identified based on Oil red O staining at varying time points (Figure 5E

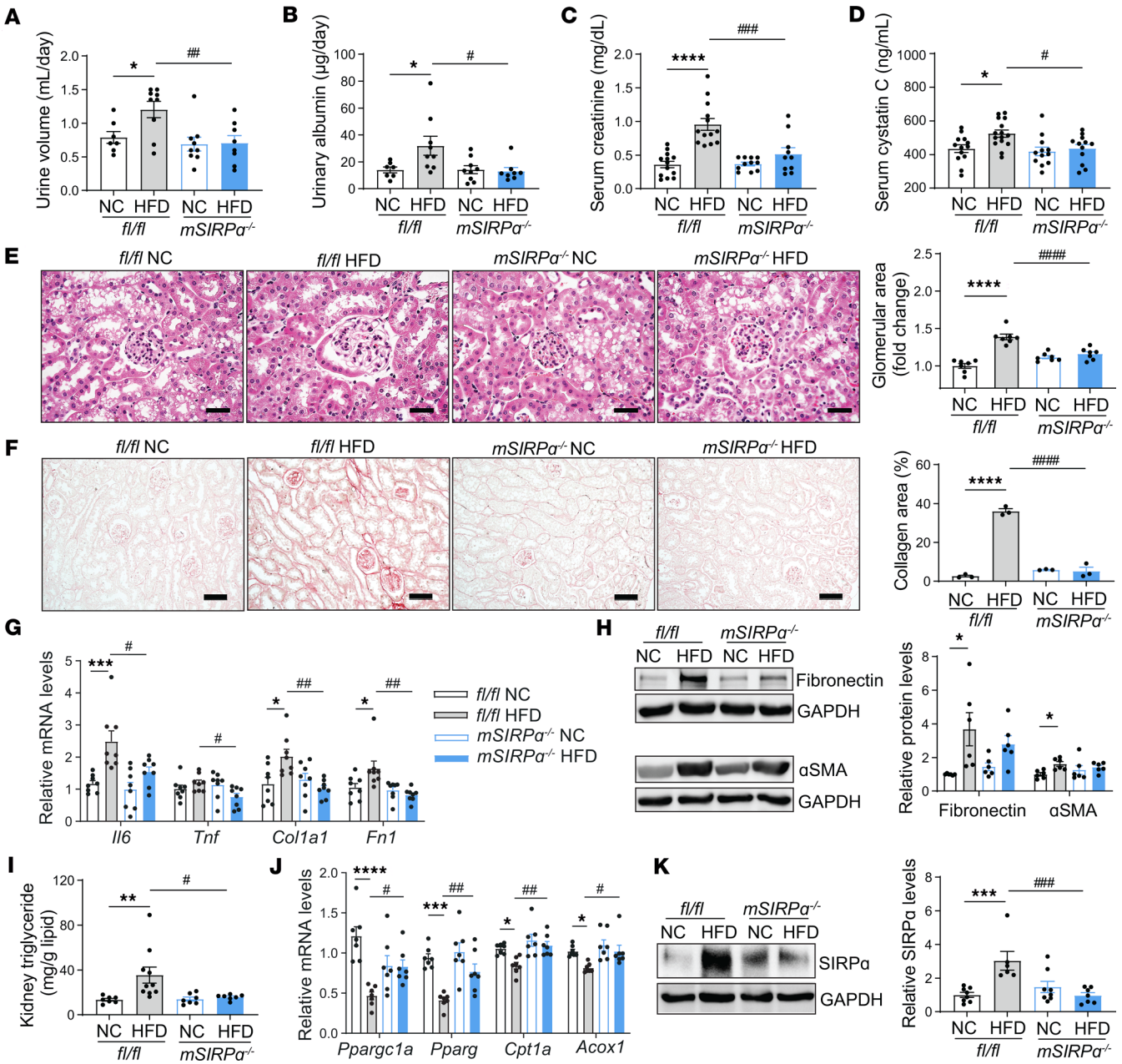

Figure 4. SIRPα suppression in skeletal muscle mitigates HFD-induced renal fibrosis and dysfunction. (**A**–**D**) After 14 weeks on high-fat diet (HFD) vs. normal chow (NC) diet, *fl/fl* and muscle-specific SIRPα-KO (*mSIRPα*$^{-/-}$) mice urine volume (n = 7–9), urinary albumin (n = 7–9), serum creatinine, and serum cystatin C (n = 10–15) were measured. (**E**) Representative H&E-stained kidney glomeruli and quantification of the glomerular size are shown (scale bar: 25 μm, n = 7). (**F**) Representative images of sirius red staining of the kidney and percentage (%) area positive for collagen are shown (scale bar: 50 μm, n = 3). (**G**) Relative mRNA levels of transcripts related to inflammation and fibrosis were determined by qPCR (n = 8). (**H**) Representative immunoblots to fibronectin and α smooth muscle actin (αSMA) and relative densities to GAPDH are identified (n = 6). (**I**) Kidney triglyceride to lipid weights were measured (n = 7–10). (**J**) Relative mRNA levels of fatty acid oxidation transcripts were determined in the kidney by qPCR (n = 7). (**K**) Representative immunoblots of SIRPα in kidney are shown. The relative SIRPα to GAPDH was determined (n = 6–8). Data are shown as mean ± SEM. Statistical significance analysis was performed using 1-way ANOVA followed by Bonferroni test for **A**–**K**. $^{*}P < 0.05$, $^{**}P < 0.01$, $^{***}P < 0.001$, $^{****}P < 0.0001$ NC vs. HFD; $^{\#}P < 0.05$, $^{\#\#}P < 0.01$, $^{\#\#\#}P < 0.001$, $^{\#\#\#\#}P < 0.0001$ *fl/fl* vs. *mSIRPα*$^{-/-}$.

and Supplemental Figure 4, D and E) along with downregulation of transcripts encoding genes responsible for FAO (Figure 5F). These results were associated with upregulation of fibronectin (*Fn1*) and collagen I (*Col1a1*) transcripts in primary proximal tubular cells after rSIRPα treatment (Figure 5G). Therefore, exogenous SIRPα reduced both ATP production and FAO transcripts with associated lipid accumulation and stimulation of genes encoding fibrosis in kidney primary proximal tubular cells.

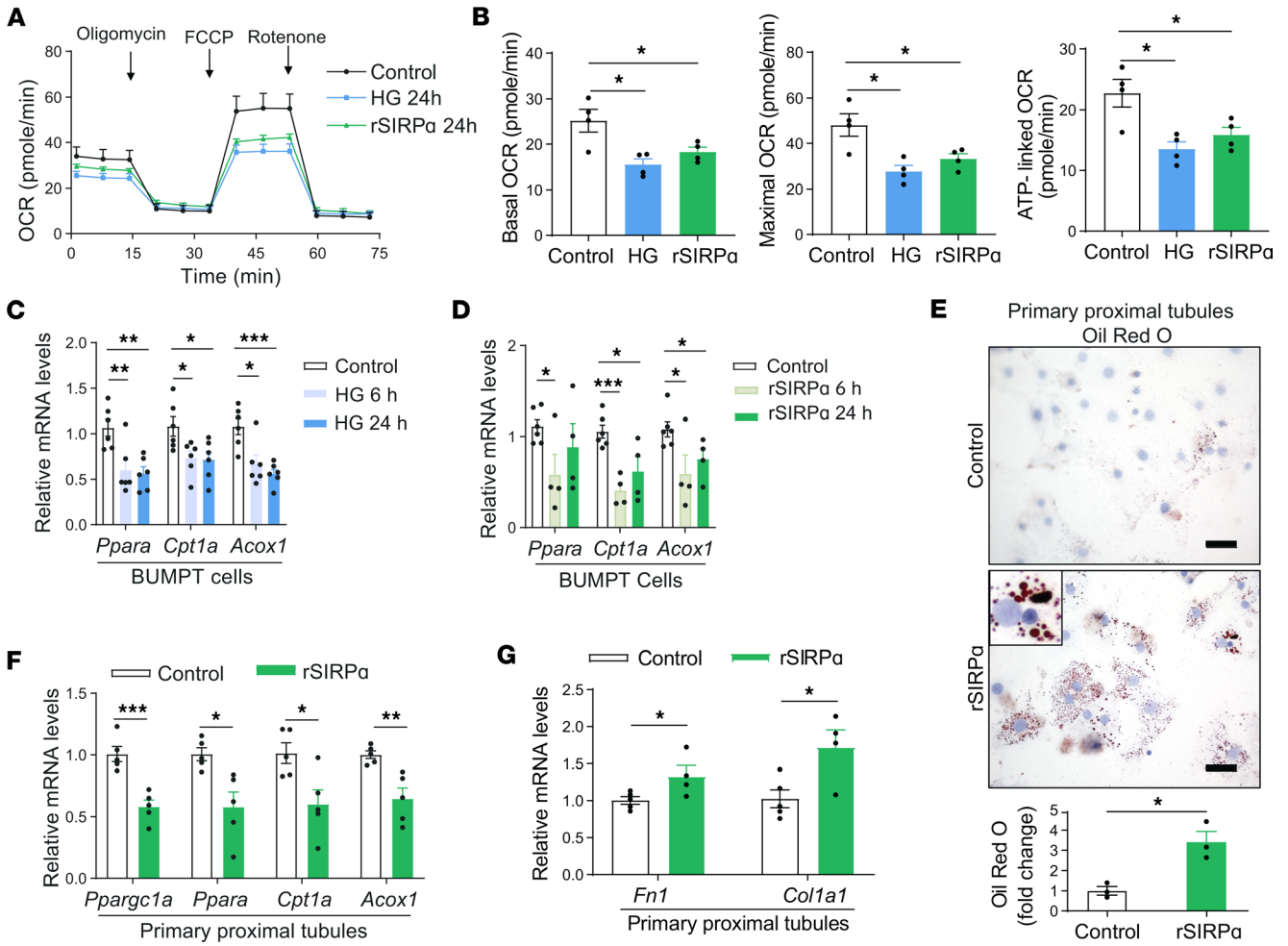

Figure 5. Recombinant SIRPα or hyperglycemia stimulates lipid accumulation in renal proximal tubular cells. (**A** and **B**) Mouse proximal tubular BUMPT cells were incubated with normal glucose (Control, 25 mM) or high glucose (HG, 75 mM) or recombinant SIRPα (rSIRPα) for 24 hours followed by cellular respiration measurements for cellular oxygen consumption rate (OCR) (**A**), basal OCR, maximal OCR, and ATP-linked respiration which were determined by a Seahorse analyzer (**B**) (n = 4). (**C**) Relative mRNA levels of fatty acid oxidation transcripts in high glucose–treated BUMPT cells (n = 6). (**D**) Relative mRNA levels of fatty acid oxidation transcripts in rSIRPα-treated BUMPT cells (n = 4–6). (**E**) Lipid accumulation was determined by Oil red O staining in kidney primary proximal tubules treated with rSIRPα for 24 h (scale bar: 25 μm, n = 3). (**F**) Relative mRNA levels of fatty acid oxidation transcripts were determined by qPCR after treatment with rSIRPα in kidney primary proximal tubules (n = 5). (**G**) Relative mRNA levels of fibrosis transcripts were determined by qPCR after treatment with rSIRPα in kidney primary proximal tubules (n = 4–5). Data are shown as mean ± SEM. Statistical significance was performed using 2-tailed unpaired t test for **B**–**G**. *P < 0.05, **P < 0.01, ***P < 0.001 Control vs. HG or rSIRPα-treated groups.

SIRPα neutralization reverses kidney FAO defects despite streptozotocin-induced hyperglycemia. To determine insulin-independent effects on kidney FAO, another model of significant hyperglycemia was utilized involving streptozotocin-induced (STZ-induced) insulinopenia. Brouwers et al. determined that STZ-induces worsens kidney function (21). In our study, 3 groups of mice (*fl/fl*, *mSIRPα*$^{-/-}$, and anti-SIRPα monoclonal antibody–treated [mAb–treated] *fl/fl* mice) were treated with STZ (Figure 6A) to induce significant hyperglycemia with blood glucose levels greater than 500 mg/dL. STZ-treated *flox* mice displayed worsening body weight and skeletal muscle losses with increased kidney weights when compared with their respective controls (Figure 6, B and C, and Supplemental Figure 5, A and B), while total body, skeletal muscle, fat, and kidney weights were improved in anti-SIRPα mAb–treated mice or *mSIRPα*$^{-/-}$ mice when compared with *flox* STZ-treated mice (Figure 6, B and C, and Supplemental Figure 5, A–C). Next, polyuria, albuminuria, blood urea nitrogen (BUN), and serum creatinine were increased in *flox* mice treated with STZ, but these parameters were significantly improved in both anti-SIRPα mAb–treated mice or *mSIRPα*$^{-/-}$ mice (Figure 6, D–G). Next, serum TG, total cholesterol (TC), kidney TG, lipid deposition (based on Oil red O staining), and glomerular size were found to be significantly reduced in STZ-treated *mSIRPα*$^{-/-}$ or anti-SIRPα mAb–treated *fl/fl* STZ mice (Figure 6,

H–L). However, in *fl/fl* STZ-treated mice, there was evidence of hypercholesterolemia, kidney lipid accumulation, and glomerulomegaly (Figure 6, H–L). Next, SIRPα proteins were found to be reduced in eWAT in *mSIRPα*$^{-/-}$ and anti-SIRPα mAb–treated mice (Supplemental Figure 5D). Additionally, fibronectin proteins were suppressed in *mSIRPα*$^{-/-}$ or anti-SIRPα mAb–treated mice despite STZ when compared with STZ-treated *fl/fl* mice (Supplemental Figure 5E). Additionally, fibrosis was increased based on sirius red and genes encoding fibrosis in STZ-treated *fl/fl* mice but significantly lower when blocking SIRPα in anti-SIRPα mAb–treated mice or *mSIRPα*$^{-/-}$ mice despite STZ (Figure 6, K and M, and Supplemental Figure 5E). Additionally, STZ suppressed renal FAO transcripts in STZ-treated *fl/fl* mice vs. their respective control mice (Figure 6M). In fact, FAO transcripts were found to be improved in *mSIRPα*$^{-/-}$ or anti-SIRPα mAb–treated mice when comparing with *fl/fl* mice after STZ treatment (Figure 6N). In conclusion, these results suggest that blocking SIRPα improved kidney fatty acid metabolism and serum creatinine while preventing features of STZ-induced kidney damage.

Diabetes stimulates circulating serum SIRPα while exogenous SIRPα suppresses kidney FAO. Finally, we examined serum samples from both diabetic and non-diabetic patients with CKD (Supplemental Table 1). On reanalysis of previous reports (5, 6) plus additional serum samples, patients with diabetes displayed a 2.0-fold significant increase in serum SIRPα (Figure 7A) when compared with nondiabetic CKD serum samples based on ELISA measurements. Therefore, human proximal tubular HK-2 cells were exposed to human rSIRPα; transcripts encoding genes responsible for FAO were suppressed with elevations in type 1 collagen (Figure 7B). Additionally, lipid droplets were increased in those human proximal tubular cells exposed to rSIRPα (Figure 7C). These results suggest that SIRPα may play an important role in human DKD, affecting kidney FAO metabolism in proximal tubules.

Discussion

This study has noteworthy clinical consequences in identifying the role of myokine SIRPα on kidney function. Muscle secretomes are underinvestigated in renal diseases, specifically the effect of the muscle directly on kidney function and its relevance in organ crosstalk. The mechanisms responsible for disruptions in lipid metabolism in kidney tubular cells in DKD remain unclear. We have determined that CKD stimulates SIRPα to impair insulin signaling in muscle (6). In this study, we examined the effects of myokine SIRPα on kidney disease. Serum SIRPα levels were elevated in patients with CKD (5, 6) and markedly increased in diabetic patients when compared to non-diabetic CKD patients.

Hirai et al. has previously identified that serum SIRPα was cleaved at its extracellular domain (ECD) producing a soluble form after parasitic infection (22). While Vladimirova et al. detected soluble SIRPα in human sera after a lipopolysaccharide (LPS) challenge, and finally Cara-Fuentes et al. detected increases in urinary SIRPα in response to CKD (23, 24). Additionally, we determined that CKD stimulates SIRPα to impair insulin signaling (6). Our current work suggests that muscle-derived SIRPα impairs lipid metabolism and kidney function in the setting of hyperglycemia. Further work is required to identify the biochemical profile including functional role and properties of serum SIRPα.

Two models of hyperglycemia were utilized, an insulin-dependent (HFD) and insulinopenic model (STZ). In our obesity-induced diabetic model, despite evidence of hyperglycemia, suppression of myokine SIRPα led to improved intracellular insulin signaling in peripheral organs with improved body weights in high fat–fed mice regardless of increased insulin levels and hyperglycemia after 13 weeks of exposure. Hyperinsulinemia is associated with weight gain, suppression of lipolysis, while stimulating lipogenesis in adipocytes (25). In fact, intracellular insulin signaling was improved despite hyperinsulinemia and no evidence of glucose lowering effects in *mSIRPα*-KO mice on HFD; therefore, the protective effects were independent of insulin or glucose levels. Improved intracellular insulin skeletal muscle signaling may affect distance organs. Further evaluations are required to determine why the protections were not insulin or glucose dependent. Moreover, thermogenic gene and adipokine expression were improved with a reduction in adipocyte area in *mSIRPα*-KO mice when compared with *flox* mice on HFD, suggesting that fat metabolism was improved. A larger adipocyte area has been reported as an independent predictor of insulin resistance (26).

Additionally, skeletal muscle metabolism was maintained in the presence of hyperglycemia upon skeletal muscle suppression of SIRPα. Skeletal muscles behave as an endocrine organ (27, 28). During exercise, myokines are secreted to communicate with distant organs to enhance fatty acid oxidation and glucose uptake (9, 29). Similar to exercise, suppression of SIRPα improved intramuscular lipid deposition and skeletal muscle losses, however, without any differences noted in oral intake or physical activity.